JOURNAL OF OLEO SCIENCE

Anti-collagenase, Anti-elastase, Anti-urease, and Anti-cancer Potentials of Isokaempferide as Natural Compound: *In vitro* and *in silico* Study

Qian Yin[1], Hao Zhang[2], Ting Huang[3], Bin Liu[4]*, Sally Negm[5], and Attalla F. El-kott[6,7]

[1] Department of Pathology, The Third Clinical Medical College of China Three Gorges University·Gezhouba Central Hospital of Sinopharm, No. 60, Qiaohu 1st Road, Xiling District, Yichang City, Hubei Province, 443002, CHINA

[2] Department of Endocrinology, The Third Clinical Medical College of China Three Gorges University·Gezhouba Central Hospital of Sinopharm, No. 60, Qiaohu 1st Road, Xiling District, Yichang City, Hubei Province, 443002, CHINA

[3] Department of Oncology, No. 215 Hospital of Shaanxi Nuclear Industry, Xianyang, No. 35, West Weiyang Road, Xianyang City, Shaanxi Province, 712000, CHINA

[4] Department of General Surgery, Dalian University Affiliated Xinhua Hospital, No. 156, Banzai Street, Shahekou District, Dalian, Liaoning Province, 116021, CHINA

[5] Department of Life Sciences, College of Science and Art Mahyel Aseer, King Khalid University, Abha 62529, SAUDI ARABIA

[6] Department of Biology, College of Science, King Khalid University, 61421 Abha, SAUDI ARABIA

[7] Department of Zoology, Faculty of Science, Damanhour University, Damanhour, 22511, EGYPT

Abstract: One of the main goals of medicinal chemistry in recent years has been the development of new enzyme inhibitors and anti-cancer medicines. The isokaempferide' ability to inhibit the enzymes urease, elastase, and collagenase were also studied. The results showed that isokaempferide was the most effective compound against the assigned enzymes, with IC_{50} values of 23.05 μM for elastase, 12.83 μM for urease, and 33.62 μM for collagenase respectively. It should be emphasized that natural compound was more effective at inhibiting some enzymes. Additionally, the compound was tested for their anti-cancer properties using colon, lung, breast cancer cell lines. The chemical activities of isokaempferide against urease, collagenase, and elastase were investigated utilizing the molecular docking study. The anti-cancer activities of the compound were evaluated against lung cancer cells such as SPC-A-1, SK-LU-1, 95D, breast cancer cells like MCF7, Hs 578Bst, Hs 319.T, and UACC-3133 cell lines, and colon cancer cell lines like CL40, SW1417, LS1034, and SW480. The chemical activities of isokaempferide against some of the expressed surface receptor proteins (EGFR, estrogen receptor, CD47, progesterone receptor, folate receptor, CD44, HER2, CD155, CXCR4, CD97, and endothelin receptor) in the mentioned cell lines were assessed using the molecular docking calculations. The results showed the probable interactions and their characteristics at an atomic level. The docking scores revealed that isokaempferide has a strong binding affinity to the enzymes and proteins. In addition, the compound formed powerful contact with the enzymes and receptors. Thus, isokaempferide could be potential inhibitor for enzymes and cancer cells.

Key words: natural compound, enzyme, colon cancer, lung cancer, *in silico* study

1 Introduction

Many medications utilized in clinical settings are derived from natural sources, and natural products play a significant part in the drug development process. A trihydroxyflavone called isokaempferide has apigenin at position 3 substituted by a methoxy group. It serves as a metabolite for plants[1]. It is both a monomethoxyflavone and a trihydroxyflavone. It shares a functional connection with an apigenin (Fig. 1). *Odontites viscosus*, *Centaurea bracteata*, and other organisms for whom data are available contain the natural substance isokaempferide. The use of natural ingredients in the formulation of skin care products is on the rise in the present day. The majority of these natural ingredients have demonstrated notable antioxidant, emollient, and ultraviolet (UV) protective properties, all of which are essential for skin care product composition[2].
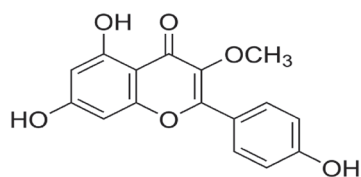
Fig. 1 Chemical structure of studied compound (Isokaempferide).

The presence of specific phytochemicals, such as an antioxidant, in the natural goods as the active component is most likely what gives the qualities. The human skin, like other organs, inexorably ages chronologically or intrinsically as a result of telomere shortening, an imbalance between free radicals and antioxidant components, hormonal changes, and environmental factors like time and genetic influence[3]. Sunlight's ultraviolet(UV)radiation also harms the skin by accelerating photoaging, also known as extrinsic skin ageing. The loss of skin firmness and suppleness as well as an increase in wrinkle creation are both effects of aging[4]. These structural changes are caused by a number of pathomechanics, such as the enzymatic breakdown and disintegration of dermal elastin fibers, which maintain the skin's resilience; the proteolytic breakdown and disorganization of dermal collagen networks, which give the skin strength and resistance; and the ongoing attacks of free radicals on skin cells, particularly mitochondrial DNA (mtDNA). The development of medicinal plants with antioxidant efficacies and inhibitory effects on the enzymes elastase and collagenase, which break down elastin and collagen fibers, may be important in slowing down the aging process of the skin[5]. Urease is a particularly promising target for both agricultural issues and clinically significant disorders like stomach ulcers and kidney stones. Urease enables Helicobacter pylori, the primary cause of peptic and gastric ulcers, to survive in the stomach's acidic environment. The hyperactivity of urease enzymes leads to the development of a range of bacterial infectious illnesses, including urolithiasis, reactive arthritis, and acute pyelonephritis[6].

The second most prevalent cancer in the world and the third most frequent cancer overall is colon cancer. Although immunotherapy and target treatments have made strides in recent years, their efficacies and applicability for advanced-stage colon cancer are still far from ideal. The most effective treatment for colon cancer is still thought to be chemotherapy[7]. Cytotoxic medications, such cisplatin and paclitaxel, can have adverse effects and increase the risk of developing chemoresistance, which puts a financial strain on patients and lowers their quality of life. Therefore, it is vitally necessary to develop a unique, highly effective anti-colon cancer agent with minimal side effects. Also, non-small cell lung cancer(NSCLC), which accounts for 80–85% of lung cancer occurrences, is the most aggres-

sive kind of lung cancer[8]. Lung cancer is one of the most deadly malignancies with a high fatality rate. With an estimated 1.8 million new cases and 1.6 million fatalities per year, lung cancer is thought to be the cause of about 20% of all cancer deaths. Due to improvements in diagnosis and treatment, the yearly drop in lung cancer mortality doubled from 2.4%(from 2009 through 2013)to 5.0%(during 2014 through 2018), and this trend is consistent with the stable decline in incidence(2.2-2.3%)[9]. The death rate for lung cancer is still high because there are no effective anti-lung cancer medications, particularly those against drug-resistant lung cancer[10]. It is critical to create new drug candidates that are highly active and effective against lung cancer, particularly treatment-resistant lung cancer. Also, the most prevalent invasive malignancy in women worldwide is breast cancer. Breast cancers account for about one-third(32%)of cancer diagnoses in female patients. It is the top cause of cancer death in women and the sixth most frequent cause of cancer-related death overall[11].

The function of most of the proteins is completed by associating with their relevant substrate or biomolecules in the body[12]. Recognizing the way that proteins associate with their substrate or activators could give crucial data for biologists. The molecular docking study is a captivating process that can be applied to selecting enzymatic substrates. Another applicability of this approach is the validation of empirical findings[13]. The molecular docking study is an adaptable method that can give these data and be utilized for finding enzymatic substrates. The evaluation of empirical results is another usefulness of molecular docking calculations, which is easily achievable[14, 15]. The features of the interactions between the chemical compound and biomolecules could be obtained at an atomic level using molecular docking[16]. This approach is a capable computer-assisted drug design that has achieved significant consideration in recent years. Furthermore, drug target prediction and knowing the molecular mechanisms can promote the drug development process.

Our aim in this study is to examine the effects of Isokaempferide as natural substance on some enzymes and cell lines and present the results in the text in the form of tables, graphs and figures.

2 Materials and Methods
2.1 Molecular docking study

The enzymes used in this study were urease(PDB ID: 4GY7), collagenase(PDB ID: 4AR1)[17], and human neutrophil elastase(PDB ID: 2Z7F)[18]. As the synthetic and natural compounds have been reported to have various benefits such as anti-cancer effects[19, 20], the anti-cancer activity of isokaempferide was evaluated against some lung cancer cells such as SPC-A-1, SK-LU-1, 95D breast cancer

cells like MCF7, Hs 578Bst, Hs 319.T, and UACC-3133 cell lines, and colon cancer cell lines like CL40, SW1417, LS1034, and SW480. The surface receptors with high expression in the mentioned cell lines were also evaluated using molecular docking. EGFR (PDB ID: 5WB7)[21] was chosen for SPC-A-1[22], estrogen receptor (PDB ID: 3OS8) was chosen for SK-LU-1 cells[23], CD47 (PDB ID: 2JJS)[24] was chosen for 95D[25], progesterone receptor (PDB ID: 1A28) was chosen for MCF7[26], folate receptor (PDB ID: 4LRH) was chosen for Hs 578Bst[27], CD44 (PDB ID: 4PZ3)[28] was chosen for Hs 319.T[27], HER2 (PDB ID: 1N8Z)[29] was chosen UACC-3133[30], CD155 (PDB ID: 3URO)[31] was chosen for CL40[32], CXCR4 (PDB ID: 3ODU)[33] was selected for SW1417[34], CD97 (PDB ID: 7DO4)[35] was selected for LS1034[36], and endothelin receptor (PDB ID: 5X93)[37] was selected for SW480[38]. The chemical activities of isokaempferide were estimated against these enzymes and proteins. The structures were gained from the PDB database (http://www.rcsb.org/pdb) and prepared using the protein preparation module of the Schrödinger Suite[39]. During the preparation of the proteins, the hydrogen atoms were added, and the molecules of water were deleted from the system. After that, an H-bond network was generated, and eventually, the system was minimized by implementing the OPLS3e force field. To achieve more dependable results, the active binding sites of the enzyme were detected using the SiteMap of Schrödinger[40], and a receptor grid was generated around the active site. The structure of isokaempferide as an SDF file was obtained from the PubChem database, and the accurate protonation states were generated by administering the LigPrep module of Schrödinger[41]. Finally, the molecular docking calculations were conducted employing the Glide of Schrödinger suites[42].

2.2 Enzymes studies

Collagenase activity was inhibited using a modified version of the technique developed by Sigma Aldrich and Thring *et al.*[43]. The experiment was carried out by combining 30 mL of sample (0-250 μg/mL in DMSO), 60 μL of buffer Tricine (50 mM, pH 7.5, contains 10 mM CaCl$_2$ and 400 mM NaCl), and 10 μL of collagenase from *Clostridium histolyticum* (Sigma C8051, USA) for the assay. 20 minutes at 37°C were spent incubating the mixes. N-[3-(2-Furyl) acryloyl]-leu-gly-Pro-Ala (Sigma F5135, USA) (1 mM in buffer Tricine) was added to 20 μL of substrate following the incubation period. Immediately after adding the substrate, the absorbance at 335 nm was measured[44].

Additionally, elastase inhibitory activity was assessed using a modified version of the Thring and Sigma Aldrich assay, with certain additions made by Widowati *et al.* 10 μL of various sample concentrations (4.17-133.33 μg/mL), 5 μL of porcine pancreatic elastase (Sigma 45124, USA) (0.5 mU/mL in cold distilled water), and 125 μL of Tris buffer were mixed together and pre-incubated for 15 minutes at

25°C. N-Sucanyl-Ala-Ala-Ala-*p*-Nitroanilide substrate [Sigma 54760, USA] was added to the mix solution and incubated for 15 minutes at 25°C. With a 410 nm wavelength, absorbance was measured immediately following incubation[45].

On the other hand, 200 μL of reaction mixture, 25 μL of Canavalia ensiformis (Jack bean) urease enzyme, 5 μL of samples of natural compound at various concentrations, and 55 μL of urea (100 mM) were incubated for 15 minutes at 30°C in 96-well plates. Then, using the indophenols method as reported by Weatherburn[46], 45 μL of phenol/sodium nitroprusside mixture (1% w/v; 0.005% w/v) and 70 μL of NaOH/NaOCl alkali mixture (0.5 w/v; 0.1 w/v) were added. Urease activity was then determined. All reactions were carried out in phosphate buffer with a pH of 6.8, and changes in absorbance were monitored for 50 minutes using an xMarkTM Microplate Spectrophotometer from BIO-RAD[47].

2.3 Anticancer activity

The test chemicals were dissolved in acetone at a concentration of 10 mM and diluted with DMEM to obtain the necessary concentrations for treating cell lines. Acetone and DMEM were given to the negative control samples in the same quantities (200 μL) as the test samples. Since the higher acetone volumes had no impact on cell proliferation when compared to the positive control samples, a normalized control was used in the study. The anti-cancer activities of the compound were evaluated against lung cancer cells such as SPC-A-1, SK-LU-1, 95D, breast cancer cells like MCF7, Hs 578Bst, Hs 319.T, and UACC-3133 cell lines, and colon cancer cell lines like CL40, SW1417, LS1034, and SW480. Overnight cell cultures in a 25 cm^2 tissue culture flask were examined under an inverted microscope. The cells were separated with trypsin and centrifuged at 1500 rpm for five minutes after being washed twice with 5 mL of PBS[48]. These 5000 cell/well rapidly growing cells were plated in 96-well plates and left to adhere for 24 hours at 37°C. After removing the media, each well received 200 μL of fresh medium containing four replicates of the test substance in various concentrations. The combination was then incubated at 37°C for 48 hours. The wells were then cleaned by adding 200 μL of PBS to each one, letting it sit for 5 minutes, and then removing it with a sterile pasture pipet. This procedure was carried out twice. For 10 minutes, the wells were treated with 100 μL of crystal violet solution. After the color was removed, the plates were washed with distilled water three times. A plate reader was used to find the absorbance at 570 nm after allowing the plates to dry at room temperature[49].

189

3 Results and Discussion

3.1 Anticancer results

An essential tactic for finding new anti-cancer medications with high efficacy and low toxicity is the development of anti-colorectal active analogs based on recognized inhibitors. Through chemical modification of the NSAIDs with promising anti-cancer actions, it is possible to completely increase the anti-cancer potency[50]. Our goal is to create novel anti-cancer drugs, and our lead molecule is isokaempferide. The compound showed good results (micromolar) for lung, breast, and colon cancer cell lines. When we examine the colon results one by one; SW480 (48.71 ± 3.93 μM) from colon cell lines had good results for isokaempferide. When we look at the colon cancer results; CL40 (52.12 ± 5.18 μM) and LS1034 (63.10 ± 6.14 μM) had the best results also. For colon cancer cell lines, IC_{50} values of isokaempferide as natural compound and 5FU are given in the following order respectively (**Fig. 2**): SW480 (48.71 ± 3.93 μg/mL) ▶ CL40 (52.12 ± 5.18 μg/mL) ▶ LS1034 (63.10 ± 6.14 μg/mL) ▶ SW1417 (77.92 ± 8.47 μg/mL) ▶ 5FU (80.51 ± 5.17 μg/mL). Also, for lung cancer cell lines, IC_{50} values of isokaempferide and 5FU are given in the following order respectively: SPC-A-1 (17.03 ± 0.94 μg/mL) ▶ 95D (21.48 ± 3.80 μg/mL) ▶ SK-LU-1 (24.08 ± 3.38 μg/mL) ▶ 5FU (27.51 ± 2.40 μg/mL).

Based on the tumor's estrogen receptor (ER) content, breast cancer can be classified as either ER-positive or ER-negative. The ER, which can encourage carcinogenesis and cancer progression in breast tissues, is expressed in about 70% of breast malignancies. In order to prevent and treat breast cancer, one of the key strategies now involves suppressing ER[51]. Tamoxifen, ethylstilbestrol, and other anti-estrogen medications are now utilized in the clinical treatment of breast cancer. E-Diethylstilbestrol is a nonsteroidal estrogen that has an estrogen-like effect and can be used to treat advanced breast cancer. It has a basic structural similarity to stilbene. Tamoxifen is the mainstay medication for ER-positive breast cancer treatment. Since it has no significant side effects, tamoxifen, a tristyrene molecule and an antiestrogen created with diethylstilbestrol estrogen as the main chemical, is frequently used in the treatment of breast cancer. The long-term use of tamoxifen, however, could result in medication resistance. Therefore, it is essential to create brand-new, powerful, and less harmful anti-breast cancer drugs for modern medicine[52]. This natural compound could be a promising agent in breast cancer therapy or drug delivery. For isokaempferide, IC_{50} values of some cancer cell lines and 5FU are given in the following order respectively (**Fig. 2**): UACC-3133 (5.03 ± 0.31 μg/mL) ▶ MCF7 (6.36 ± 0.40 μg/mL) ▶ Hs 319.T (7.26 ± 0.85 μg/mL) ▶ Hs 578Bst (9.30 ± 1.04 μg/mL) ▶ 5FU (12.21 ± 1.23 μg/mL).

3.2 Enzymes results

A class of ECM-degrading enzymes known as matrix metalloproteinases (MMPs) includes collagenase and elastase. They are crucial to tissue remodeling and healing. They have a significant role in the control of extracellular matrix deposition and breakdown, which is necessary for the re-epithelialization of wounds[53]. Elastase and collagenase play important roles in wound development and repair as well as the pathophysiology of numerous diseases, including cancer, cardiovascular disease, inflammation, bone degeneration, and fibrosis[54]. The obtained data demonstrated that the natural compound, isokaempferide with IC_{50} values of 92.24, 106.50, and 16.88 μM exhibited good inhibitory effects for collagenase, elastase, and urease enzymes. For all enzymes, IC_{50} values of isokaempferide are given in the following order (**Fig. 2**): Urease (16.88 ± 1.55 μg/mL) ▶ collagenase (92.24 ± 7.68 μg/mL) ▶ elastase (106.50 ± 5.11 μg/
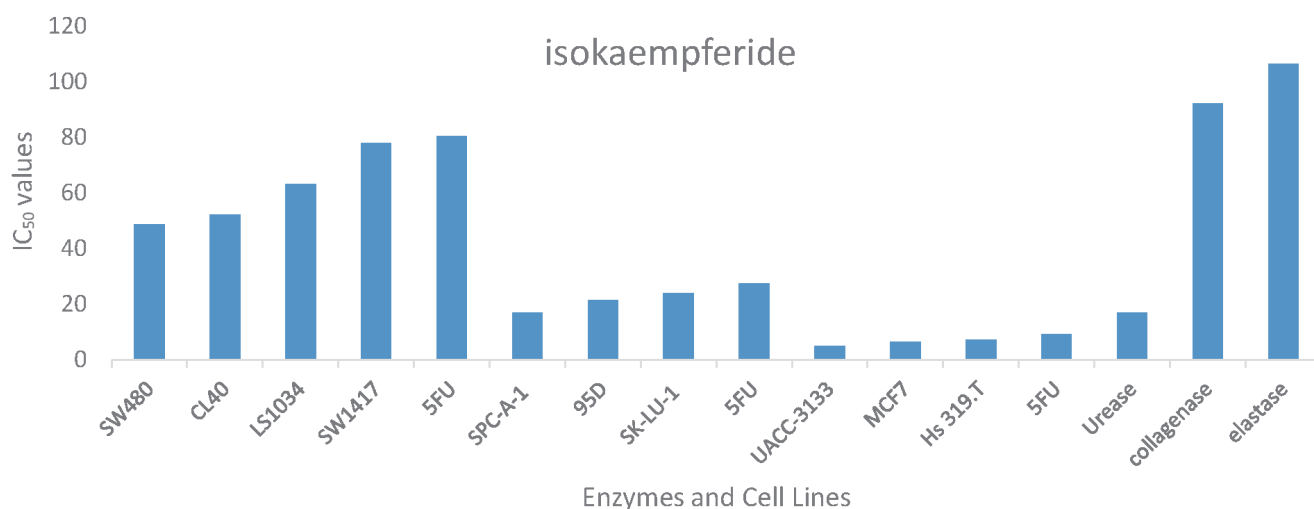

Fig. 2 IC_{50} values of enzymes and cell lines. (5FU was studied in different diluted solutions for each cancer).

mL). Both collagenase and elastase are important enzymes that aid in the breakdown of supporting and connective proteins in skin tissue, including collagen and elastin, respectively. Despite the fact that these degenerations are normal processes of healthy skin aging, excessive hyperactivity or overexpression of collagenase and elastase are frequently brought on by both external causes (such as UV radiation) and internal cellular oxidative stress. The aggravation of collagen and elastin protein breakdown in skin tissue significantly contributes to the loss of skin mechanical structures and ultimately results in the production of skin wrinkles. Small compounds produced from natural products that have inhibitory effects on the collagenase and elastase enzymes are therefore candidates for use as cosmeceutical anti-wrinkle treatments[55]. To determine whether combinations of isokaempferide may exert synergistic anti-collagenase and anti-elastase effects, we evaluated the inhibitory effects of isokaempferide on collagenase and elastase enzymes. We also used computational and biochemical assays to determine the skin permeability of isokaempferide. Additionally, since these investigations have resulted in the discovery of medications effective in a number of physiological circumstances, studies on enzyme inhibition continue to be an important area of pharmaceutical research. Inhibitors of enzymes can interact with them to prevent their action toward natural substrates. Recently, urease inhibitors have drawn a lot of interest as potential novel anti-ulcer medications. Ironically, urease was the first enzyme to crystallize, albeit little is still known about how it works[56].

3.3 Molecular docking

The chemical activities of isokaempferide when interacting with the enzymes (urease, collagenase, and elastase) and proteins (EGFR, estrogen receptor, CD47, progesterone receptor, folate receptor, CD44, HER2, CD155, CXCR4, CD97, and endothelin receptor) were evaluated performing the molecular docking calculations. The outcomes showed the probable residues of the biomolecules that can create strong interactions with the compound. The docking pose of isokaempferide among the residues of urease is shown in Fig. 3A. The interactions between isokaempferide and urease are displayed in Fig. 3A. As could be seen in Fig. 3A, isokaempferide has created two hydrogen bonds with the residues of urease. These residues are Val8 and Asn15. There are also some other interactions, which increase the binding affinity of isokaempferide to the enzyme. The residues with these interactions are Val8, Glu9, and Gly12.

The docking pose of isokaempferide amongst the residues of collagenase is shown in Fig. 3B. Indeed, Isokaempferide has created six hydrogen bonds with collagenase. These residues are Lys375, Asp388, Lys389, Asp397, Leu400, and Tyr695. The length of these hydrogen bonds is presented in Table 1. This compound has also created a Pi-Pi T-shaped, Pi-alkyl, and some other contacts with the residues Lys353, Tyr460, and Lys641 of collagenase. Figure 3C shows the docking pose of isokaempferide among the residues of elastase. There are two hydrogen bonds between the compound and the residues of elastase, which are Arg178, and Asn180. There are also two other contacts between this compound and the residues Arg129 and Cys168. Figure 3D represents the docking pose of isokaempferide among the residues of CD44. Isokaempferide has created three hydrogen bonds and some other contacts with the residues of CD44. The residues with hydrogen bonds are Ile26, Glu37, and Arg90. The other contacts are created between the compound and residues Arg41 and Cys77.

The docking pose of isokaempferide among the residues of CD47 is presented in Fig. 4A. Isokaempferide has created three hydrogen bonds with the residues of CD47. These residues are Ser85, Asp86, and Ser89. This compound has created some other contacts with CD47 residues. These residues are Asp62 and His90. Figure 4B displays the docking pose of isokaempferide among the residues of EGFR. There are four hydrogen bonds between isokaempferide and EGFR. These residues are Lys4, Asn86, Arg231, and Tyr251. There are also other interactions between this compound and EGFR residues. These residues are Val6, Val36, Leu38, Ala62, Thr249, and Ala265. The docking pose of isokaempferide among the residues of the estrogen receptor is displayed in Fig. 4C. There are four hydrogen bonds between isokaempferide and the residues of the estrogen receptor. These residues are Glu353, Arg394, and two bonds are created between the compound and Met421. There are also some other kinds of interactions between isokaempferide and residues Leu346, Ala350, Leu387, Leu391, Phe404, and Ile424. The docking pose of isokaempferide among the residues of folate receptor is presented in Fig. 4D. Isokaempferide has constructed seven hydrogen bonds with the residues of folate receptor. These residues are Ser57, and Asp81, two bonds with Arg103, two bonds with His135, and Ser174. There are also other interactions between this compound and residues Tyr60, Trp64, Tyr85, and Trp171. Figure 5A shows the docking pose of isokaempferide among the residues of HER2. The results show that isokaempferide has created two hydrogen bonds with the HER2 residues. These residues are Gly270 and Cys289. Moreover, there are three residues that have created some contacts with isokaempferide. These residues are Tyr281 and Leu291.

The docking pose of isokaempferide among the residues of progesterone receptor is displayed in Fig. 5B. The results indicate that isokaempferide has constructed three hydrogen bonds with the residues Leu758, Ile699, and Gln815. There are also other interactions such as Pi-Alkyl contacts and carbon-hydrogen bonds between isokaempferide and the residues of the progesterone receptor. These
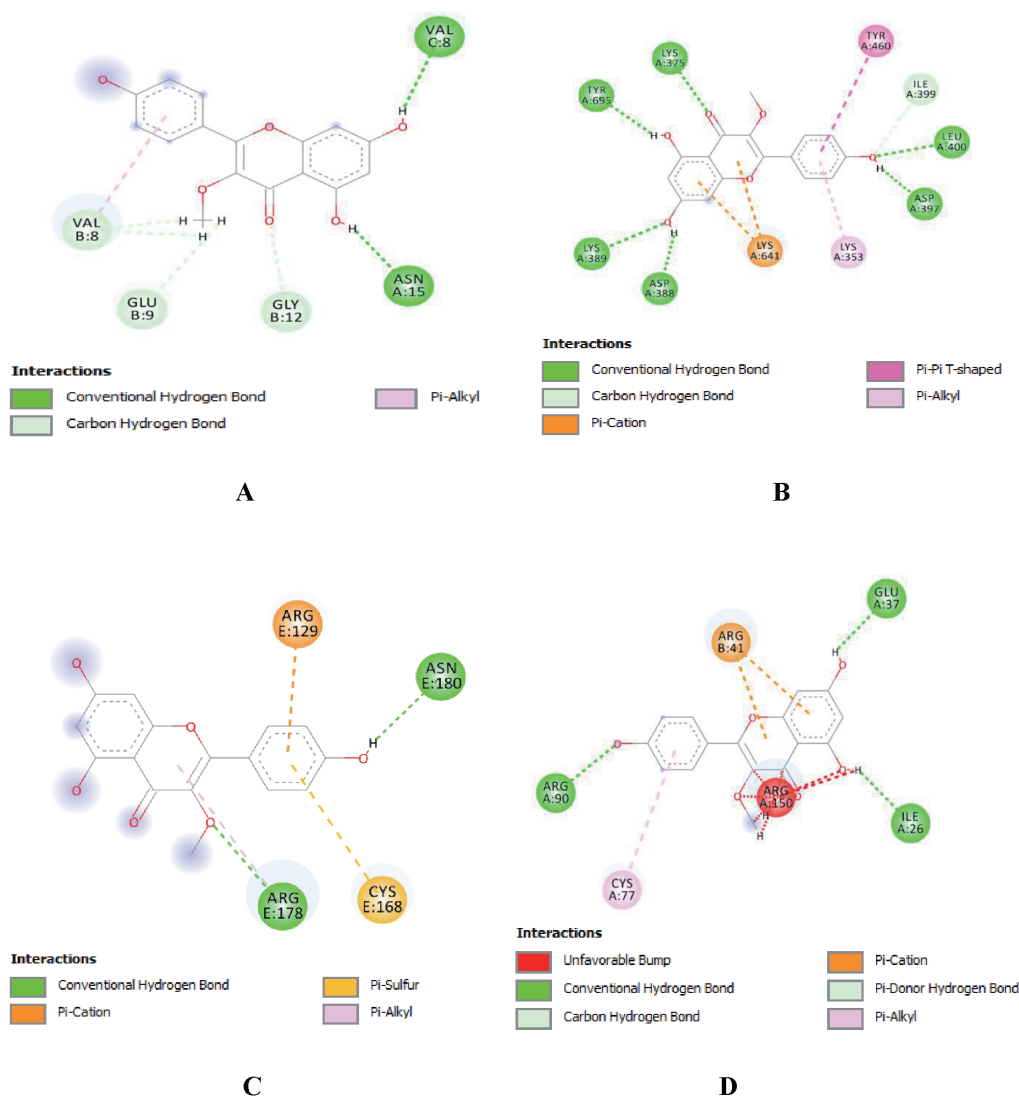
A

B

C

D

Fig. 3 A) The interactions of Isokaempferide and urease. Dashed lines indicate the constructed bonds between the ligand and enzyme. B) The interactions of Isokaempferide and collagenase. Green dashed lines indicate the hydrogen bonds. C) The interactions of Isokaempferide and elastase. The dashed lines indicate the constructed bonds between the ligand and enzyme. D) The interactions of Isokaempferide and CD44. The dashed lines indicate the constructed bonds between the ligand and enzyme.

Table 1 The docking scores and H-bonds length obtained from the molecular docking calculations for enzymes.

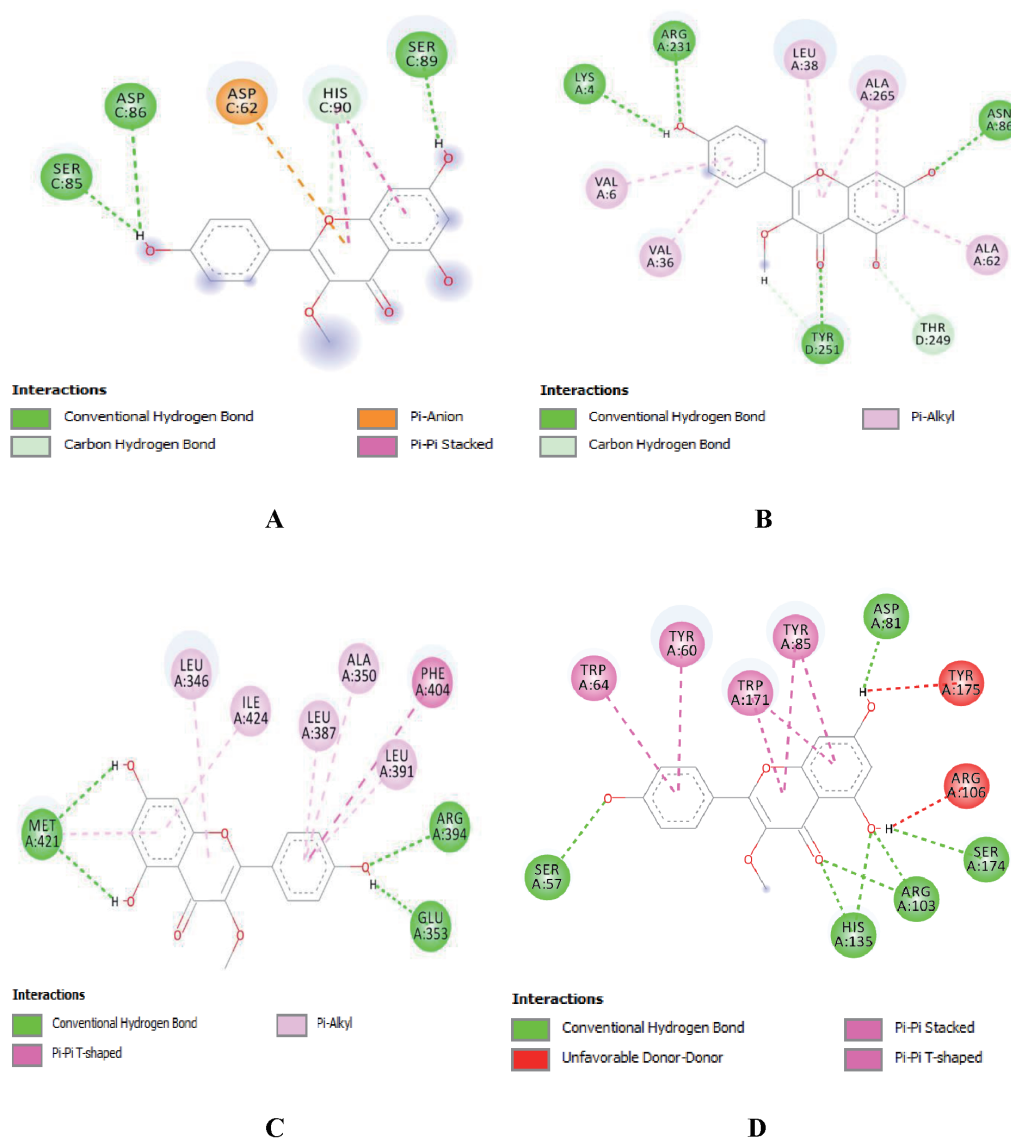| Compound	Parameter	Urease	Collagenase	Elastase
	IC_{50} (μM)	16.88	92.24	106.50
	Docking score (kcal/mol)	− 4.988	− 5.565	− 1.816
Isokaempferide	Residues with H-bond and their length	Val8:2.08Å Asn15:1.81Å	Lys375: 2.05Å Asp388: 1.81Å Lys389: 2.74Å Asp397: 1.63Å Leu400: 2.49Å Tyr695: 2.37Å	Arg178: 2.15Å Asn180: 1.99Å

Fig. 4 A) The interactions of Isokaempferide and CD47. The dashed lines indicate the constructed bonds between the ligand and protein. B) The interactions of Isokaempferide and EGFR. The dashed lines indicate the constructed bonds between the ligand and protein. C) The interactions of Isokaempferide and estrogen receptor. The dashed lines indicate the constructed bonds between the ligand and protein. D) The interactions of Isokaempferide and folate receptor. The dashed lines indicate the constructed bonds between the ligand and protein.

residues are Pro696, Val698, Trp765, Arg766, and Lys769. The docking pose of isokaempferide among the residues of CD97 is presented in Fig. 5C. Isokaempferide has constructed two hydrogen bonds with the residues of CD97. These residues are Trp29 and Cys62. The length of these bonds is presented in Table 4. There are also two other contacts with the residues Trp29 and Pro31. The docking pose of isokaempferide among the residues of CD155 is presented in Fig. 5D. isokaempferide has constructed one hydrogen bond with the residues of CD155. This residue is Leu103. There are also five other contacts between the compound and the residues of CD155. These residues are

Val30, Leu51, Val53, Pro129, and Gly131. The docking pose of isokaempferide among the residues of CXCR4 is presented in Fig. 6A. Isokaempferide has constructed four hydrogen bonds with the residues Asp187, Arg188, His203, and Glu288 of CXCR4. There are also some other interactions between isokaempferide and the residues of the receptor. These residues are Tyr190, Val196, and Gln200.

The docking pose of isokaempferide among the residues of the endothelin receptor is presented in Fig. 6B. Isokaempferide has constructed one hydrogen bond with the residue Cys255 of this receptor. There are also some other interactions between the endothelin receptor residues and
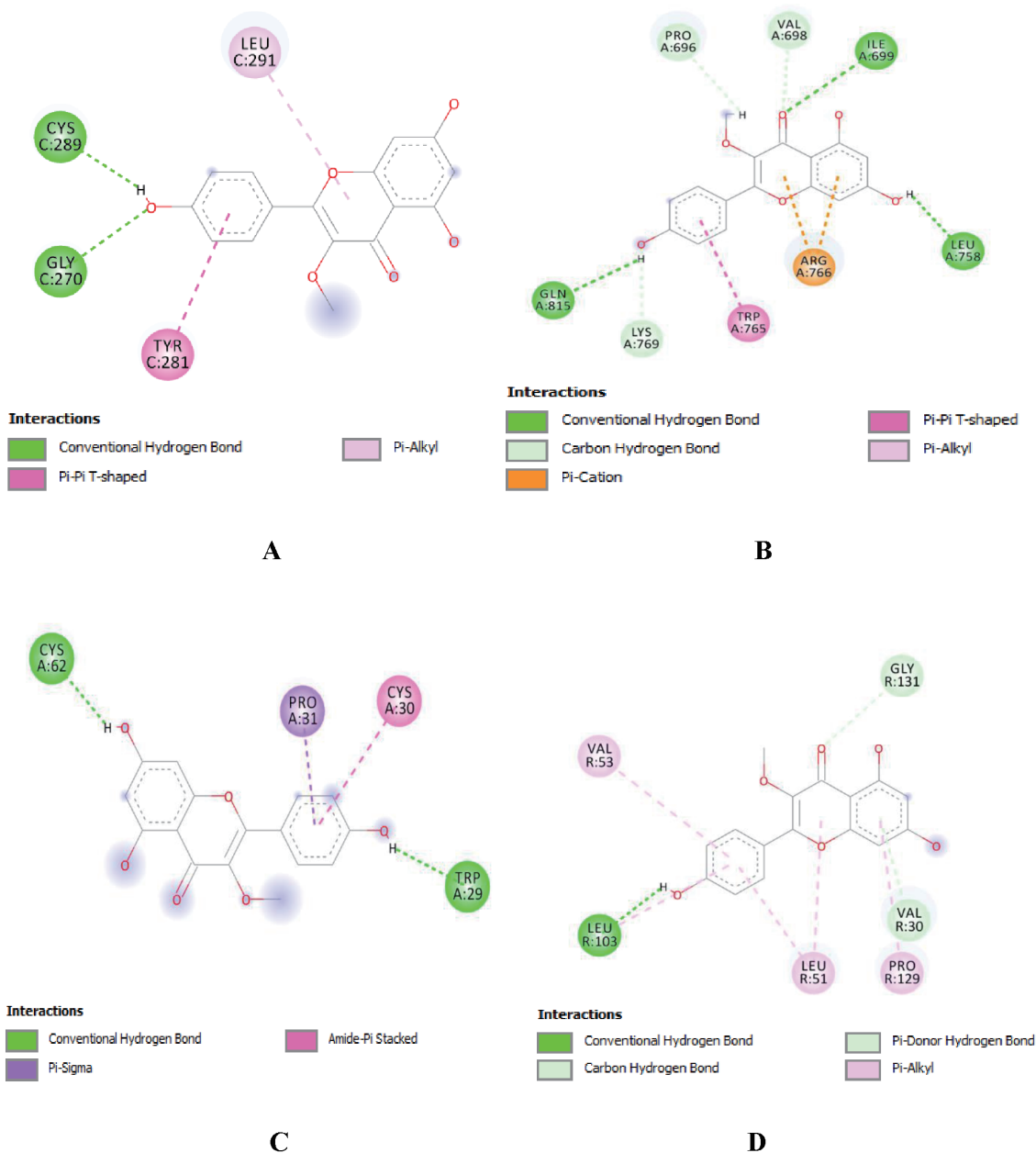
Fig. 5 A) The interactions of Isokaempferide and HER2. The dashed lines indicate the constructed bonds between the ligand and protein. B) The interactions of Isokaempferide and progestrone receptor. The dashed lines indicate the constructed bonds between the ligand and protein. C) The interactions of Isokaempferide and CD97. The dashed lines indicate the constructed bonds between the ligand and protein. D) The interactions of Isokaempferide and CD155. The dashed lines indicate the constructed bonds between the ligand and protein.

isokaempferide. These residues are His150, Val177, Pro178, and Gln181. The details of these interactions are shown in Figures of supplementary file. In addition to determining the probable interactions between isokaempferide and biomolecules, the molecular docking study can provide the binding affinity of the ligands to the biomolecules. The docking score reveals this affinity. This value for the ligand-protein complexes discussed above is shown in Tables 1 to

4. Although isokaempferide is s useful inhibitor against these enzymes and cancer cells, this compound has to be delivered to the target site. A satisfactory solution for this problem is vesicular nanocarriers, which develop their effects[57, 58].
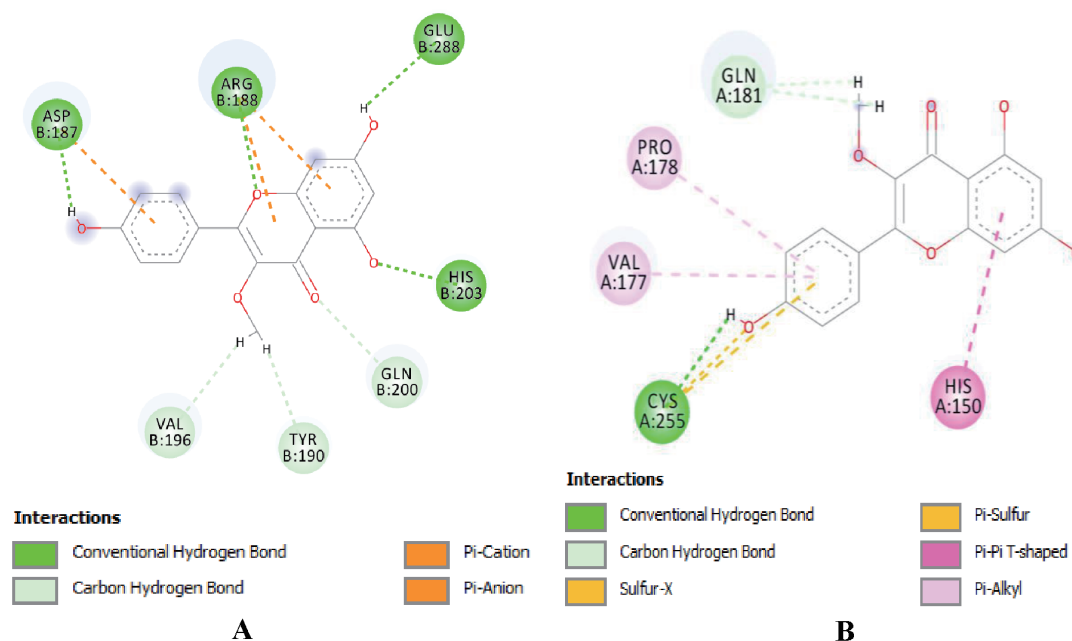
Fig. 6 A) The interactions of Isokaempferide and CXCR4. The dashed lines indicate the constructed bonds between the ligand and protein. B) The interactions of Isokaempferide and endothelin receptor. The dashed lines indicate the constructed bonds between the ligand and protein.

Table 2 The docking scores and H-bonds length obtained from the molecular docking calculations for anti-lung cancer effects (EGFR, estrogen receptor, and CD47).

Compound	Parameter	EGFR (SPC-A-1)	Estrogen receptor (SK-LU-1)	CD47 (95D)
	IC$_{50}$ (μM)	17.03	24.08	21.48
	Docking score (kcal/mol)	−7.467	−8.616	−2.796
Isokaempferide	Residues with H-bond and their length	Lys4:3.04Å Asn86:2.16Å Arg231:2.27Å Tyr251:1.90Å	Glu353:1.59Å Arg394:2.18Å Met421:2.85Å	Ser85:2.08Å Asp86:3.06Å Ser89:2.03Å

Table 3 The docking scores and H-bonds length obtained from the molecular docking calculations for anti-breast cancer effects (progesterone receptor, folate receptor, CD44, and HER2).

Compound	Parameter	Progesterone receptor (MCF7)	Folate receptor (Hs 578Bst)	CD44 (Hs 319.T)	HER2 (UACC-3133)
	IC$_{50}$ (μM)	6.36	9.30	7.26	5.03
	Docking score (kcal/mol)	−4.107	−9.135	−4.505	−5.106
Isokaempferide	Residues with H-bond and their length	Ile699:2.54Å Leu758:2.09Å Gln815:2.75Å	Ser57:2.69Å Asp81:1.65Å Arg103:1.78Å Arg103:2.41Å His135:1.79Å His135:2.72Å Ser174:2.22Å	Ile26:2.02Å Glu37:1.93Å Arg90:2.08Å	Gly270:2.29Å Cys289:1.88Å

Table 4 The docking scores and H-bonds length obtained from the molecular docking calculations for Anti-colon cancer effects (CD155, CXCR4, CD97, and endothelin receptor).

Compound	Parameter	CD155 (CL40)	CXCR4 (SW1417)	CD97 (LS1034)	Endothelin receptor (SW480)
Isokaempferide	IC$_{50}$ (µM)	52.12	77.92	63.10	48.71
	Docking score (kcal/mol)	−5.844	−4.130	−2.603	−5.418
	Residues with H-bond and their length	Leu103:1.85Å	Asp187:1.67Å Arg188:2.32Å His203:1.65Å Glu288:2.10Å	Trp29:1.84Å Cys62:1.85Å	Cys255:2.39Å

4 Conclusions

In silico examinations could be performed as proper tools to interpret the results of empirical research. These strategies can deliver insight into the interactions in a more precise view. Among different methods, molecular docking has attracted more attention because of its capability to define the possible interactions between the ligands and biomolecules at an atomic level. In this study, molecular docking was conducted to assess the activities of iso-kaempferide against hyaluronidase, collagenase, and elastase. For all enzymes, IC$_{50}$ values of isokaempferide are given in the following order: Urease (16.88 ± 1.55 µg/mL) ▶ collagenase (92.24 ± 7.68 µg/mL) ▶ elastase (106.50 ± 5.11 µg/mL). The activities of this compound were also analyzed against eight expressed surface receptor proteins (EGFR, estrogen receptor, CD47, progesterone receptor, folate receptor, CD44, HER2, CD155, CXCR4, CD97, and endothelin receptor) in the lung cancer cells such as SPC-A-1, SK-LU-1, 95D, breast cancer cells like MCF7, Hs 578Bst, Hs 319.T, and UACC-3133 cell lines, and colon cancer cell lines like CL40, SW1417, LS1034, and SW480. The results suggested that isokaempferide could be considered a possible inhibitor for the mentioned enzymes and cancer cell lines.

Acknowledgment

Conflicts of Interest

No other potential conflicts of interest relevant to this article were reported.

Supporting Information

This material is available free of charge via the Internet at doi: 10.5650/jos.ess23176

References

1) Johnson, T.O.; Adegboyega, A.E.; Ojo, O.A.; Yusuf, A.J.; Iwaloye, O. *et al.* A Computational approach to elucidate the interactions of chemicals from *Artemisia annua* targeted toward SARS-CoV-2 main protease inhibition for COVID-19 treatment. *Front. Med* (Lausanne). **15**, 907583 (2022).

2) Lin, S.R.; Chang, C.H.; Hsu, C.F.; Tsai, M.J.; Cheng, H. *et al.* Natural compounds as potential adjuvants to cancer therapy: Preclinical evidence. *Br. J. Pharmacol.* **177**, 1409-1423 (2020).

3) Marijan, M.; Tomić, D.; Strawa, J.W.; Jakupović, L.; Inić, S. *et al.* Optimization of cyclodextrin-assisted extraction of phenolics from *Helichrysum italicum* for preparation of extracts with anti-elastase and anti-collagenase properties. *Metabolites* **13**, 257 (2023).

4) Yücel, Ç.; Karatoprak, G.Ş.; Yalçıntaş, S.; Böncü, T.E. Ethosomal (−)-epigallocatechin-3-gallate as a novel approach to enhance antioxidant, anti-collagenase and anti-elastase effects. *Beilstein J. Nanotechnol.* **13**, 491-502 (2022).

5) Azahar, N.F.; Abd Gani, S.S.; Zaidan, U.H.; Bawon, P.; Halmi, M.I.E. Optimization of the antioxidant activities of mixtures of Melastomataceae leaves species (*M. malabathricum* Linn Smith, *M. decemfidum*, and *M. hirta*) using a Simplex Centroid Design and their anti-collagenase and elastase properties. *Appl. Sci.* **10**, 7002 (2020).

6) Dawar, K.; Fahad, S.; Jahangir, M.M.R.; Munir, I.; Alam, S.S. *et al.* Biochar and urease inhibitor mitigate NH$_3$ and N$_2$O emissions and improve wheat yield in a urea fertilized alkaline soil. *Sci. Rep.* **11**, 17413 (2021).

7) Yan, X.Q.; Wang, Z.C.; Zhang, B.; Qi, P.F.; Li, G.G. *et al.* Dihydropyrazole derivatives containing benzo oxygen heterocycle and sulfonamide moieties selectively and

potently inhibit COX-2: design, synthesis, and anti-colon cancer activity evaluation. *Molecules* **24**, 1685（2019）.

8）Rudin, C.M.; Poirier, J.T.; Byers, L.A.; Dive, C.; Dowlati, A. *et al.* Molecular subtypes of small cell lung cancer: a synthesis of human and mouse model data. *Nat. Rev. Cancer* **19**, 289-297（2019）.

9）Zhao, H.; Maruthupandy, M.; Al-mekhlafi, F.A.; Chackaravarthi, G.; Ramachandran, G. Biological synthesis of copper oxide nanoparticles using marine endophytic actinomycetes and evaluation of biofilm producing bacteria and A549 lung cancer cells. *J. King Saud Univ. Sci.* **34**, 101866（2022）.

10）Song, P.; Zhao, F.; Li, D.; Qu, J.; Yao, M. *et al.* Synthesis of selective PAK4 inhibitors for lung metastasis of lung cancer and melanoma cells. *Acta Pharm. Sin. B* **12**, 2905-2922（2022）.

11）Cui, Y.M.; Li, W.; Shen, T.Z.; Tao, Y.X.; Liu, B.Q. *et al.* Design, synthesis and anti-breast cancer evaluation of biaryl pyridine analogues as potent RSK inhibitors. *Bioorg. Med. Chem. Lett.* **59**, 128565（2022）.

12）Mihăşan, M. What *in silico* molecular docking can do for the ʻbench-working biologistsʼ. *J. Biosci.* **37**, 1089-1095（2012）.

13）Poustforoosh, A.; Hashemipour, H.; Pardakhty, A.; Kalantari Pour, M. Preparation of nano-micelles of meloxicam for transdermal drug delivery and simulation of drug release: A computational supported experimental study. *Can. J. Chem. Eng.* **100**, 3428-3436（2022）.

14）B-Rao, C.; Subramanian, J.; Sharma, S.D. Managing protein flexibility in docking and its applications. *Drug Discov. Today* **14**, 394-400（2009）.

15）Hagar, M.; Ahmed, H.A.; Aljohani, G.; Alhaddad, O.A. Investigation of some antiviral N-heterocycles as COVID 19 drug: Molecular docking and DFT calculations. *Int. J. Mol. Sci.* **21**, 3922（2020）.

16）Meng, X.Y.; Zhang, H.X.; Mezei, M.; Cui, M. Molecular docking: A powerful approach for atructure-based drug discovery. *Curr. Comput. Aided Drug Des.* **7**, 146-157（2012）.

17）Eckhard, U.; Schönauer, E.; Brandstetter, H. Structural basis for activity regulation and substrate preference of clostridial collagenases G, H, and T. *J. Biol. Chem.* **288**, 20184-20194（2013）.

18）Koizumi, M.; Fujino, A.; Fukushima, K.; Kamimura, T.; Takimoto-Kamimura, M. Complex of human neutrophil elastase with 1/2SLPI. *J. Synchrotron Radiat.* **15**, 308-311（2008）.

19）Sargazi, M.L.; Juybari, K.B.; Tarzi, M.E.; Amirkhosravi, A.; Nematollahi, M.H. *et al.* Naringenin attenuates cell viability and migration of C6 glioblastoma cell line: A possible role of hedgehog signaling pathway. *Mol. Biol. Rep.* **48**, 6413-6421（2021）.

20）Mehrabani, M.; Raeiszadeh, M.; Najafipour, H.; Esmaeli Tarzi, M.; Amirkhosravi, A. *et al.* Evaluation of the cytotoxicity, antibacterial, antioxidant, and anti-inflammatory effects of different extracts of *Punica granatum* var. pleniflora. *J. Kerman Univ. Med. Sci.* **27**, 414-425（2020）.

21）Freed, D.M.; Bessman, N.J.; Kiyatkin, A.; Salazar-Cavazos, E.; Byrne, P.O. *et al.* EGFR ligands differentially stabilize receptor dimers to specify signaling kinetics. *Cell* **171**, 683-695（2017）.

22）Xu, N.; Zhang, X.; Wang, X.; Ge, H.Y.; Wang, X.Y. *et al.* FoxM1 mediated resistance to gefitinib in non-small-cell lung cancer cells. *Acta Pharmacol. Sin.* **33**, 675-681（2012）.

23）Rodriguez-Lara, V.; Ignacio, G.S.; Cerbón Cervantes, M.A. Estrogen induces CXCR4 overexpression and CXCR4/CXL12 pathway activation in lung adenocarcinoma cells *in vitro*. *Endocr. Res.* **42**, 219-231（2017）.

24）Hatherley, D.; Graham, S.C.; Turner, J.; Harlos, K.; Stuart, D.I. *et al.* Paired receptor specificity explained by structures of signal regulatory proteins alone and complexed with CD47. *Mol. Cell* **31**, 266-277（2008）.

25）Chiang, Z.C.; Fang, S.; Shen, Y.K.; Cui, D.; Weng, H. *et al.* Development of novel CD47-specific ADCs possessing high potency against non-small cell lung cancer *in vitro* and *in vivo*. *Front. Oncol.* **12**, 857927（2022）.

26）Bajalovic, N.; Or, Y.Z.; Woo, A.R.E.; Lee, S.H.; Lin, V.C.L. High levels of progesterone receptor B in MCF-7 cells enable radical anti-tumoral and anti-estrogenic effect of progestin. *Biomedicines* **10**, 1860（2022）.

27）Gupta, U.; Saren, B.N.; Khaparkhuntikar, K.; Madan, J.; Singh, P.K. Applications of lipid-engineered nanoplatforms in the delivery of various cancer therapeutics to surmount breast cancer. *J. Control. Release* **348**, 1089-1115（2022）.

28）Liu, L.K.; Finzel, B. High-resolution crystal structures of alternate forms of the human CD44 hyaluronan-binding domain reveal a site for protein interaction. *Acta Crystallogr. F Struct. Biol.* **70**, 1155-1161（2014）.

29）Wang, C.; Deng, S.; Chen, J.; Xu, X.; Hu, X. *et al.* The synergistic effects of pyrotinib combined with adriamycin on HER2-positive breast cancer. *Front. Oncol.* **11**, 616443（2021）.

30）Sflomos, G.; Schipper, K.; Koorman, T.; Fitzpatrick, A.; Oesterreich, S. *et al.* Atlas of lobular breast cancer models: Challenges and strategic directions. *Cancers* **13**, 5396（2021）.

31）Zhang, P.; Mueller, S.; Morais, M.C.; Bator, C.M.; Bowman, V.D. *et al.* Crystal structure of CD155 and electron microscopic studies of its complexes with polioviruses. *Proc. Natl. Acad. Sci. U.S.A.* **105**, 18284-18289（2008）.

32) Al-Yassiry, K.A.R. The effect of curcumin on CD155 gene expression in colorectal carcinoma. *Ann. Romanian Soc. Cell Biol.* **25**, 3(2021).

33) Wu, B.; Chien, E.Y.; Mol, C.D.; Fenalti, G.; Liu, W. *et al.* Structures of the CXCR4 chemokine GPCR with small-molecule and cyclic peptide antagonists. *Science* **330**, 1066-1071(2010).

34) Sala, R.; Rioja-Blanco, E.; Serna, N.; Sánchez-García, L.; Álamo, P. *et al.* GSDMD-dependent pyroptotic induction by a multivalent CXCR4-targeted nanotoxin blocks colorectal cancer metastases. *Drug delivery* **29**, 1384-1397(2022).

35) Niu, M.; Xu, S.; Yang, J.; Yao, D.; Li, N. *et al.* Structural basis for CD97 recognition of the decay-accelerating factor CD55 suggests mechanosensitive activation of adhesion GPCRs. *J. Biol. Chem.* **296**, 100776(2021).

36) Steinert, M.; Wobus, M.; Boltze, C.; Schütz, A.; Wahlbuhl, M. *et al.* Expression and regulation of CD97 in colorectal carcinoma cell lines and tumor tissues. *Am. J. Pathol.* **161**, 1657-1667(2002).

37) Shihoya, W.; Nishizawa, T.; Yamashita, K.; Inoue, A.; Hirata, K. *et al.* X-ray structures of endothelin ETB receptor bound to clinical antagonist bosentan and its analog. *Nat. Struct. Mol. Biol.* **24**, 758-764(2017).

38) Haque, S.U.; Dashwood, M.R.; Heetun, M.; Shiwen, X.; Farooqui, N. *et al.* Efficacy of the specific endothelin a receptor antagonist zibotentan(ZD4054)in colorectal cancer: A preclinical study. *Mol. Cancer Ther.* **12**, 1556-1567(2013).

39) Poustforoosh, A.; Faramarz, S.; Nematollahi, M.H.; Hashemipour, H.; Negahdaripour, M. *et al. In silico* SELEX screening and statistical analysis of newly designed 5mer peptide-aptamers as Bcl-xl inhibitors using the Taguchi method. *Comput. Biol. Med.* **146**, 105632(2022).

40) Beg, M.A.; Athar, F. Computational method in COVID-19: Revelation of preliminary mutations of RdRp of SARS CoV-2 that build new horizons for therapeutic development. *J. Hum. Virol. Retrovirol.* **8**, 62-72 (2020).

41) Poustforoosh, A.; Hashemipour, H.; Tüzün, B.; Azadpour, M.; Faramarz, S. *et al.* The impact of D614G mutation of SARS-COV-2 on the efficacy of anti-viral drugs: A comparative molecular docking and molecular dynamics study. *Curr. Microbiol.* **79**, 1-12(2022).

42) Poustforoosh, A.; Faramarz, S.; Nematollahi, M.H.; Hashemipour, H.; Tüzün, B. *et al.* 3D-QSAR, molecular docking, molecular dynamics, and ADME/T analysis of marketed and newly designed flavonoids as inhibitors of Bcl-2 family proteins for targeting U-87 glioblastoma. *J. Cell. Biochem.* **123**, 390-405(2022).

43) Tamsyn, S.A.; Thring, P.H.; Naughton, D.P. Anti-collagenase, anti-elastase and anti-oxidant activities of extracts from 21 plants. *BMC Complement. Altern. Med.* **9**, 1-11(2009).

44) Thabet, A.A.; Ayoub, I.M.; Youssef, F.S.; Al Sayed, E.; Singab, A.N.B. Essential oils from the leaves and flowers of *Leucophyllum frutescens*(Scrophulariaceae): Phytochemical analysis and inhibitory effects against elastase and collagenase *in vitro*. *Nat. Prod. Res.* **36**, 4698-4702(2021).

45) Andrade, J.M.; Domínguez-Martín, E.M.; Nicolai, M.; Faustino, C.; Rodrigues, L.M. *et al.* Screening the dermatological potential of plectranthus species components: Antioxidant and inhibitory capacities over elastase, collagenase and tyrosinase. *J. Enzyme Inhib. Med. Chem.* **36**, 258-270(2021).

46) Weatherburn, M. Phenol-hypochlorite reaction for determination of ammonia. *Anal. Chem.* **39**, 971-974 (1967).

47) Han, S.; Wang, Y. Synthesis, characterization and crystal structures of Schiff base copper complexes with urease inhibitory activity. *Acta Chim. Slov.* **68**, 961-969(2021).

48) Das, S.; Diyali, S.; Vinothini, G.; Perumalsamy, B.; Balakrishnan, G. *et al.* Synthesis, morphological analysis, antibacterial activity of iron oxide nanoparticles and the cytotoxic effect on lung cancer cell line. *Heliyon* **6**, e04953(2020).

49) Tombuloglu, H.; Khan, F.A.; Almessiere, M.A.; Aldakheel, S.; Baykal, A. Synthesis of niobium substituted cobalt-nickel nano-ferrite(Co0. 5Ni0. 5NbxFe2-xO4(x ≤ 0.1)by hydrothermal approach show strong anti-colon cancer activities. *J. Biomol. Struct. Dyn.* **39**, 2257-2265(2021).

50) Chen, J.; Chen, Z.; Tan, L.; Yang, J.; Shen, L. *et al.* Synthesis of a new chlorin photosensitizer for photodynamic therapy against colon cancer. *Mater. Chem. Front.* **6**, 1129-1136(2022).

51) Song, Y.Y.; Xia, K.; Wu, X.Q.; Zeng, C.G.; Tang, S.A. *et al.* Design, synthesis, and anti-breast cancer activity evaluation of endoperoxide-type pyrido/pyrrolo[2,3-d]pyrimidine derivatives. *J. Heterocycl. Chem.* **60**, 1138-1149(2023).

52) Al-Owaidi, M.F.; Mahdi, M.F. Synthesis and anti-breast cancer activity evaluation of the designed chlorobenzothiophene derivatives: Promising estrogen receptor alpha inhibitors. *Egypt. J. Chem.* **66**, 431-441(2023).

53) Deniz, F.S.S.; Salmas, R.E.; Emerce, E.; Cankaya, I.I.T.; Yusufoglu, H.S. *et al.* Evaluation of collagenase, elastase and tyrosinase inhibitory activities of *Cotinus coggygria* Scop. through *in vitro* and *in silico* approaches. *S. Afr. J. Bot.* **132**, 277-288(2020).

54) Hering, A.; Stefanowicz-Hajduk, J.; Gucwa, M.; Wielgomas, B.; Ochocka, J.R. Photoprotection and antiaging activity of extracts from Honeybush(*Cyclopia* sp.)— *In vitro* wound healing and inhibition of the skin extracellular matrix enzymes: Tyrosinase, collagenase,

198

elastase and hyaluronidase. *Pharmaceutics* **15**, 1542 （2023）.

55）Chang-Ho, E.; Kang, M.S.; Kim, I.J. Elastase/collagenase inhibition compositions of *Citrus unshiu* and its association with phenolic content and anti-oxidant activity. *Appl. Sci.* **10**, 4838（2020）.

56）Korona-Glowniak, I.; Glowniak-Lipa, A.; Ludwiczuk, A.; Baj, T.; Malm, A. The *in vitro* activity of essential oils against *Helicobacter pylori* growth and urease activity. *Molecules* **25**, 586（2020）.

57）Poustforoosh, A.; Nematollahi, M.H.; Hashemipour, H.; Pardakhty, A. Recent advances in Bio-conjugated nanocarriers for crossing the Blood-Brain Barrier in （pre-）clinical studies with an emphasis on vesicles. *J.*

Control. Release **343**, 777-797（2022）.

58）Asadikaram, G.; Poustforoosh, A.; Pardakhty, A.; Torkzadeh-Mahani, M.; Nematollahi, M.H. Niosomal virosome derived by vesicular stomatitis virus glycoprotein as a new gene carrier. *Biochem. Biophys. Res. Commun.* **534**, 980-987（2020）.